

# Solvent Effects and Mechanism for a Nucleophilic Aromatic Substitution from QM/MM Simulations

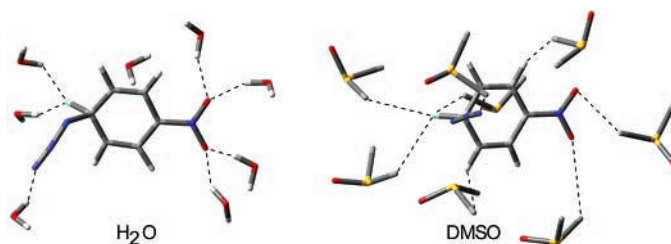
Orlando Acevedo and William L. Jorgensen\*

Department of Chemistry, Yale University, 225 Prospect Street,  
New Haven, Connecticut 06520-8107

william.jorgensen@yale.edu

Received May 13, 2004

## ABSTRACT

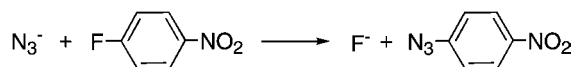


The nucleophilic aromatic substitution ( $S_NAr$ ) reaction between azide ion and 4-fluoronitrobenzene has been investigated using QM/MM and DFT/PCM calculations in protic and dipolar aprotic solvents. The effects of solvation on the transition structures, the intermediate Meisenheimer complex, and the rate of reaction are elucidated. The large rate increases in proceeding from protic to dipolar aprotic solvents are only reproduced by the QM/MM methodology.

Aromatic nucleophilic substitution reactions have been proposed to proceed through an addition–elimination mechanism ( $S_NAr$ ) involving the formation of an intermediate Meisenheimer complex.<sup>1–3</sup> Previous mechanistic investigations have included examination of the effects of nucleophile strength, leaving group ability, and solvation.<sup>4–16</sup> The rates

of  $S_NAr$  reactions with anionic nucleophiles are particularly sensitive to medium effects, proceeding far faster in dipolar aprotic than protic solvents.<sup>3</sup> As an initial computational study of an  $S_NAr$  reaction in solution, the reaction between azide ion and 4-fluoronitrobenzene (Scheme 1) has been

**Scheme 1.**  $S_NAr$  Reaction between Azide Ion and 4-Fluoronitrobenzene



investigated in water, methanol, acetonitrile, and DMSO. Besides testing the methodology, transition structures and intermediates in solution and the origin of the solvent effects on the reaction rate are elucidated. This  $S_NAr$  reaction was

- (1) Bunnett, J. F.; Zahler, R. E. *Chem. Rev.* **1951**, 49, 273–412.
- (2) Miller, J.; Parker, A. J. *J. Am. Chem. Soc.* **1961**, 83, 117–123.
- (3) Parker, A. J. *Chem. Rev.* **1969**, 69, 1–32.
- (4) Bunnett, J. F.; Garbisch, E. W., Jr.; Pruitt, K. M. *J. Am. Chem. Soc.* **1957**, 79, 385–391.
- (5) Alexander, R.; Ko, E. C. F.; Parker, A. J.; Broxton, T. J. *J. Am. Chem. Soc.* **1968**, 90, 5049–5069.
- (6) Cox, B. G.; Parker, A. J. *J. Am. Chem. Soc.* **1973**, 95, 402–407.
- (7) Cox, B. G.; Parker, A. J. *J. Am. Chem. Soc.* **1973**, 95, 408–410.
- (8) Broxton, T. J.; Muir, D. M.; Parker, A. J. *J. Org. Chem.* **1975**, 40, 3230–3233.
- (9) Takabe, T.; Takenaka, K.; Yamaguchi, K.; Fueno, T. *Chem. Phys. Lett.* **1976**, 44, 65–69.
- (10) Forlani, L.; Boga, C.; Forconi, M. *J. Chem. Soc., Perkin Trans. 2* **1999**, 1455–1458.
- (11) Dotterer, S. K.; Harris, R. L. *J. Org. Chem.* **1988**, 53, 777–779.
- (12) Bacaloglu, R.; Bunton, C. A.; Oretga, F. *J. Am. Chem. Soc.* **1989**, 111, 1041–1047.
- (13) Simkin, B. Y.; Gluz, E. B.; Glukhovtsev, M. N.; Minkin, V. I. *J. Mol. Struct. (THEOCHEM)* **1993**, 284, 123–137.

- (14) Arvanites, A. C.; Boerth, D. W. *J. Mol. Model* **2001**, 7, 245–256.
- (15) Tascioglu, S.; Gurdere, M. B. *Colloids Surf., A* **2000**, 173, 101–107.
- (16) Persson, J.; Matsson, O. *J. Org. Chem.* **1998**, 63, 9348–9350.

chosen owing to the availability of corresponding experimental kinetic data.<sup>7</sup>

Mixed quantum and molecular mechanical (QM/MM) calculations<sup>17,18</sup> were carried out with BOSS.<sup>19</sup> The QM method for the reacting system is PDDG/PM3, which has been extensively validated for the gas phase<sup>20</sup> and has yielded excellent results for  $S_N2$  reactions in solution.<sup>21</sup> The solvent molecules were represented with the united-atom OPLS force field<sup>22</sup> for the nonaqueous solvents and with the TIP4P water model.<sup>23</sup> To locate the minima and maxima on the free energy surface for the reaction, a two-dimensional free energy map was constructed. Free-energy perturbation (FEP) calculations were performed in conjunction with Metropolis Monte Carlo (MC) simulations at 25 °C and 1 atm. The systems consisted of the reactants, plus 395 solvent molecules for the nonaqueous solvents or 740 molecules for water. For the solute atoms, unscaled partial charges were obtained from the CM3 charge model<sup>24</sup> and the PDDG/PM3 wave function. Solute–solvent and solvent–solvent intermolecular cutoff distances of 12 Å were employed. Changes in free energy were calculated for perturbing the distance between the closest nitrogen of the azide and the attacked carbon of 4-fluoronitrobenzene ( $R_{NC}$ ) and the distance between the fluorine and the reacting carbon ( $R_{CF}$ ); see Figure 1.



**Figure 1.** Bond length variables,  $R_{CF}$  and  $R_{NC}$ , in the  $S_NAr$  reaction between azide ion and 4-fluoronitrobenzene.

The initial ranges for  $R_{NC}$  and  $R_{CF}$  were 1.35–2.35 Å with an increment of 0.05 Å. Each simulation consisted of 2.5 M configurations of equilibration followed by 5 M configurations of averaging. As an example, the resultant map for the reaction in water is shown in Figure 2. In all cases, transition structures for the addition (TS1) and elimination (TS2) steps and the intermediate complex were readily located.

To locate the critical points more precisely, the regions surrounding the free energy minimum and maxima from the

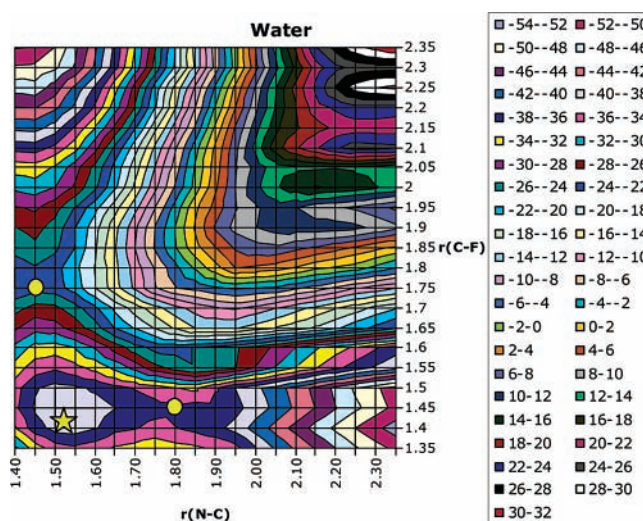


**Figure 2.** Two-dimensional potential of mean force in water. ☆ marks the intermediate complex, and O symbols mark the transition structures. All distances in Å and energies in kcal/mol.

initial maps were explored using increments of 0.01 Å. This provided refined results for the reaction in the four solvents, as summarized in Table 1.

**Table 1.** Computed Bond Lengths (Å) for Transition Structures and Intermediate Complex (IC) at 25 °C and 1 atm

|                    |          | ts1  | ic   | ts2  |
|--------------------|----------|------|------|------|
| H <sub>2</sub> O   | $R_{CF}$ | 1.41 | 1.44 | 1.82 |
|                    | $R_{NC}$ | 1.79 | 1.52 | 1.44 |
| CH <sub>3</sub> OH | $R_{CF}$ | 1.40 | 1.45 | 1.84 |
|                    | $R_{NC}$ | 1.84 | 1.52 | 1.45 |
| CH <sub>3</sub> CN | $R_{CF}$ | 1.41 | 1.43 | 1.96 |
|                    | $R_{NC}$ | 1.96 | 1.52 | 1.45 |
| DMSO               | $R_{CF}$ | 1.41 | 1.44 | 2.01 |
|                    | $R_{NC}$ | 1.96 | 1.52 | 1.45 |

Normal expectation would be that azide and fluoride ion are better solvated in the protic solvents, so the first TS should be later (shorter  $R_{NC}$ ) and the second TS earlier (shorter  $R_{CF}$ ) in water and methanol than in acetonitrile and DMSO.<sup>5</sup> This pattern is apparent in the results in Table 1 with the typical difference in bond lengths near 0.15 Å. Consistent with the earlier elimination TS in the protic solvents, the QM/MM charges on fluorine in TS2 are −0.58, −0.59, −0.67 and −0.76 for water, methanol, acetonitrile and DMSO, respectively. An experimental estimate of the charge on fluorine in the transition state is also ca. −0.6 for the reaction in DMF.<sup>3</sup>

Activation barriers and the relative free energy of the intermediate were computed by extending  $R_{NC}$  to 5 Å and smoothly connecting the reactants, transition structures, and intermediate using increments of 0.02 Å (Table 2, Figure 3). Uncertainties in the free energy values are calculated by

- (17) Warshel, A.; Levitt, M. *J. Mol. Biol.* **1976**, *103*, 227–249.
- (18) Kaminski, G. A.; Jorgensen, W. L. *J. Phys. Chem. B* **1998**, *102*, 1787–1796.
- (19) Jorgensen, W. L. *BOSS*, Version 4.5; Yale University: New Haven, CT, 2003.
- (20) Repasky, M. P.; Chandrasekhar, J.; Jorgensen, W. L. *J. Comput. Chem.* **2002**, *23*, 1601–1622. Tubert-Brohman, I.; Guimarães, C. R. W.; Repasky, M. P.; Jorgensen, W. L. *J. Comput. Chem.* **2003**, *25*, 138–150.
- (21) Vayner, G.; Houk, K. N.; Jorgensen, W. L.; Brauman, J. I. *J. Am. Chem. Soc.* **2004**, *126*, in press.
- (22) Jorgensen, W. L. *J. Phys. Chem.* **1986**, *90*, 1276–1284.
- (23) Jorgensen, W. L.; Chandrasekhar, J.; Madura, J. D.; Impey, W.; Klein, M. L. *J. Chem. Phys.* **1983**, *79*, 926–935.
- (24) Thompson, J. D.; Cramer, C. J.; Truhlar, D. G. *J. Comput. Chem.* **2003**, *24*, 1291–1304.

**Table 2.** Free Energies,  $\Delta G$  (kcal/mol), Relative to Reactants for the  $S_NAr$  Reaction from MC/QM/MM Simulations

|                    | ts1  | ic    | ts2  | exptl <sup>a</sup> |
|--------------------|------|-------|------|--------------------|
| H <sub>2</sub> O   | 30.8 | 18.1  | 35.3 | 28.1               |
| CH <sub>3</sub> OH | 26.1 | 10.6  | 27.5 | 27.5               |
| CH <sub>3</sub> CN | 17.5 | -2.94 | 21.1 | 21.8               |
| DMSO               | 17.0 | -5.02 | 19.9 | 21.8               |

<sup>a</sup> Free energies of activation from ref 7.

propagating the standard deviation ( $\sigma_i$ ) on each individual  $\Delta G_i$ .<sup>25,26</sup> The smooth free-energy profiles were accompanied by statistical uncertainties ( $1\sigma$ ) of only 0.005–0.03 kcal/mol in each window; thus, the overall uncertainties in the computed free energies of activation,  $\Delta G^\ddagger$ , are below 0.6 kcal/mol ( $0.03^2 \times 400$  windows)<sup>1/2</sup>. The computed  $\Delta G^\ddagger$  values for either TS are in reasonable agreement with the experimental data and reproduce well the large rate accelerations in progressing from the protic to the dipolar aprotic solvents.

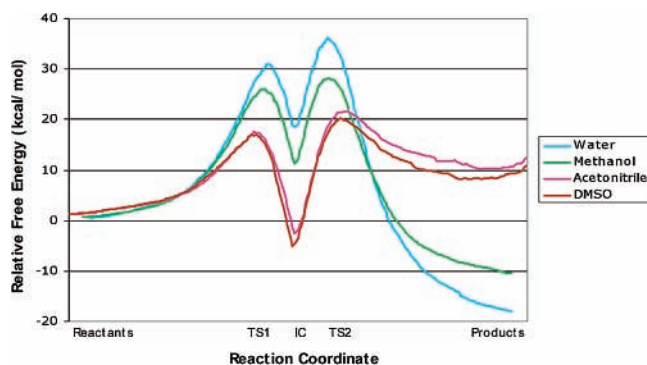


**Figure 3.** Potentials of mean force for the  $S_NAr$  reaction in the four solvents from the MC/QM/MM calculations.

There has been discourse on whether the rate-limiting step is for the addition of the nucleophile<sup>3,10,27,28</sup> or elimination of the leaving group,<sup>1,4,29,30</sup> or whether it may switch depending on the solvent.<sup>2,8,31</sup> The MC/QM/MM calculations find that the elimination step (TS2) has the highest barrier in all solvents. However, semiempirical QM methods overestimate the activation barriers for  $S_N2$  reactions in which fluoride is the nucleophile or the leaving group.<sup>21</sup> To examine

this concern, density functional theory (DFT) was also applied to the  $S_NAr$  reaction. Specifically, the B3LYP functional<sup>32,33</sup> and the 6-31+G(d) basis set were used to characterize the transition structures and the intermediate in a vacuum using Gaussian03.<sup>34</sup> Frequency calculations provided zero-point and thermal corrections, and the effect of solvent was approximated by subsequent single-point calculations using the polarizable continuum model (PCM)<sup>35</sup> with a larger basis set, 6-311+G(2d,p). Dielectric constants of 78.39, 32.63, 36.64, and 46.7 were used for water, methanol, acetonitrile, and DMSO.

The  $\Delta G^\ddagger$  values computed using DFT/PCM for TS1 in the protic solvents agree well with experiment (Table 3),

**Table 3.** Free Energies,  $\Delta G$  (kcal/mol), Relative to Reactants for the  $S_NAr$  Reaction from B3LYP/6-311+G(2d,p) and PCM Calculations

|                    | ts1  | ic   | ts2  | exptl <sup>a</sup> |
|--------------------|------|------|------|--------------------|
| H <sub>2</sub> O   | 27.6 | 25.1 | 16.4 | 28.1               |
| CH <sub>3</sub> OH | 27.9 | 25.6 | 17.4 | 27.5               |
| CH <sub>3</sub> CN | 27.1 | 24.9 | 16.9 | 21.8               |
| DMSO               | 27.9 | 25.5 | 17.5 | 21.8               |

<sup>a</sup> Free energies of activation from ref 7.

and TS1 is predicted to be rate-determining in all cases. However, the high dielectric constants lead the DFT/PCM results to be basically the same in the four solvents, and the observed, substantial solvent effects on the activation barrier are not reproduced. The observed variability of the stability of the intermediate in different media is also not reflected in the DFT/PCM results.<sup>2,3</sup> In contrast, the MC/QM/MM calculations find the intermediate to be similar in free energy to the reactants in the dipolar aprotic solvents, whereas it has relative free energies of 11 and 18 kcal/mol in methanol and water (Figure 3). The higher free energies for the products than reactants in the dipolar aprotic solvents (Figure 3) indicate that in the absence of a counterion or trace water to stabilize the fluoride ion, net conversion would be minimal. The explicit representation of solvent molecules and hydrogen bonding in the MC/QM/MM methodology leads to the improved results for the solvent effects; however, the differences between the MC/QM/MM and DFT/PCM results leave open the question on the rate-controlling step.

In the thermodynamic analysis of Cox and Parker,<sup>7</sup> the origin of the lower free energies of activation for the  $S_NAr$  reaction in the dipolar aprotic solvents relative to methanol is enthalpically dominated about equally from poorer solvation of the azide ion and better solvation of the transition state. Detailed insights on the changes in solvation along the reaction paths are also available from the MC/QM/MM calculations. In particular, the solute–solvent energy pair

(25) Repasky, M. P.; Guimarães, C. R. W.; Chandrasekhar, J.; Tirado-Rives, J.; Jorgensen, W. L. *J. Am. Chem. Soc.* **2003**, *125*, 6663–6672.

(26) Guimarães, C. R. W.; Repasky, M. P.; Chandrasekhar, J.; Tirado-Rives, J.; Jorgensen, W. L. *J. Am. Chem. Soc.* **2003**, *125*, 6892–6899.

(27) Chen, W. J.; Graminski, G. F.; Armstrong, R. N. *Biochemistry* **1988**, *27*, 647–654.

(28) Zheng, Y.; Ornstein, R. L. *J. Am. Chem. Soc.* **1997**, *119*, 648–655.

(29) Parker, A. J. *Organic Sulfur Compounds*; Pergamon Press: Oxford, England, 1961; Vol. 1.

(30) Tanaka, K.; Deguchi, M.; Iwata, S. *J. Chem. Res., Synop.* **1999**, 528–529.

(31) Persson, J.; Axelsson, S.; Matsson, O. *J. Am. Chem. Soc.* **1996**, *118*, 20–23.

(32) Becke, A. D. *J. Chem. Phys.* **1993**, *98*, 5648–5652.

(33) Lee, C.; Yang, W.; Parr, R. G. *Phys. Rev.* **1988**, *37*, 785–789.

(34) Frisch, M. J. et al. *Gaussian 03*, Revision A.1; Gaussian, Inc.: Pittsburgh, PA, 2003. [Full reference given in Supporting Information].

(35) Tomasi, J.; Persico, M. *Chem. Rev.* **1994**, *94*, 2027–2094.

distributions record the average number of solvent molecules that interact with the solute and the associated energy. The results for the  $S_NAr$  reaction in water are shown in Figure 4; the results for the other solvents can be found in

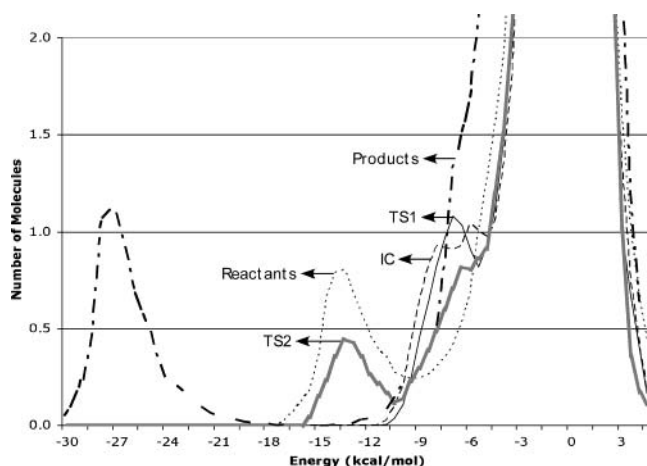


**Figure 4.** Solute-solvent energy pair distributions for the  $S_NAr$  reaction in water. The ordinate records the number of water molecules that interact with the solutes with their interaction energy on the abscissa. Units for the ordinate are number of molecules per kcal/mol.

Supporting Information. Hydrogen bonding in protic solvents is reflected in the left-most region, with interaction energies more attractive than ca.  $-5$  kcal/mol. The large band near  $0$  kcal/mol results from the many distant solvent molecules in outer shells.

The outstanding features in Figure 4 are the low-energy peaks for the reactants and product, which arise from the water molecules that are hydrogen-bonded to the azide and fluoride ions. Integration of the bands centered near  $-14$  and  $-27$  kcal/mol yields 6.3 and 6.0 water molecules with the stronger interactions for the more charge-localized fluoride ion. Loss of the hydrogen bonding with azide ion in progressing to TS1 is clearly a major contributor to the activation barrier; TS2 is then helped by the emerging

hydration of fluoride ion, though the band centered near  $-13$  kcal/mol only contains 3 water molecules. In acetonitrile, the corresponding band for the reactant is shifted much to the right, has its maximum at  $-7.5$  kcal/mol, and integrates to 8–9 acetonitrile molecules up to  $-5$  kcal/mol. The band for solvation of the product fluoride ion is more distinct, peaks at  $-10.6$  kcal/mol, and contains 6–7 acetonitrile molecules. Solvation of the charge-delocalized TS1 in the different media appears similar in these distributions, the IC is more like TS1 than TS2, and TS2 does yield a well-defined low-energy band representing the strong interactions with the emerging fluoride in each case. These results point to the poorer solvation of azide ion in the dipolar aprotic solvents as the principal contributor to the enhanced reaction rates in comparison with protic solvents.

In conclusion, MC/QM/MM simulations have been applied to a  $S_NAr$  reaction with good success in reproducing the observed solvent effects on the activation barrier. The generally accepted addition/elimination mechanism was found in all cases. The intermediate Meisenheimer complex was computed to be more stable relative to the reactants in aprotic than protic solvents, which is consistent with spectroscopic observations for related systems.<sup>36,37</sup> The importance of variations in specific solute-solvent interactions along the reaction paths is evident in energy-pair distributions such as Figure 4 and in the failure of DFT/PCM calculations to reproduce the rate retardation in hydrogen-bonding solvents. The lower rates are attributed primarily to greater differential stabilization of azide ion than the more charge delocalized transition structures via hydrogen bonding in water and methanol.

**Acknowledgment.** Gratitude is expressed to the National Science Foundation and the National Institutes of Health for support of this research.

**Supporting Information Available:** Optimized gas-phase structures and energies for TS1, TS2, and IC, and additional energy pair distributions. This material is available free of charge via the Internet at <http://pubs.acs.org>.

OL049121K

(36) Strauss, M. J. *Chem. Rev.* **1970**, *70*, 667–712.

(37) Bernasconi, C. F. *Acc. Chem. Res.* **1978**, *11*, 147–152.